

Kernel Representation and Similarity Measure for Incomplete Data

Yang Cao
Tsinghua University,
Great Bay University
Guangdong, China
charles.cao@ieee.org

Sikun Yang
Great Bay University
Guangdong, China

Kai He
Dongguan University of Technology
Guangdong, China

Wenjun Ma
South China Normal University
Guangdong, China

Ming Liu
Deakin University
VIC, Australia

Yuju Yang
Tsinghua University
Guangdong, China

Jian Weng
Jinan University
Guangdong, China

Abstract

Measuring similarity between incomplete data is a fundamental challenge in web mining, recommendation systems, and user behavior analysis. Traditional approaches either discard incomplete data or perform imputation as a preprocessing step, leading to information loss and biased similarity estimates. This paper presents the proximity kernel, a new similarity measure that directly computes similarity between incomplete data in kernel feature space without explicit imputation in the original space. The proposed method introduces data-dependent binning combined with proximity assignment to project data into a high-dimensional sparse representation that adapts to local density variations. For missing value handling, we propose a cascading fallback strategy to estimate missing feature distributions. We conduct clustering tasks on the proposed kernel representation across 12 real world incomplete datasets, demonstrating superior performance compared to existing methods while maintaining linear time complexity. All the code are available at <https://anonymous.4open.science/r/proximity-kernel-2289>.

CCS Concepts

• **Do Not Use This Code** → **Generate the Correct Terms for Your Paper**; *Generate the Correct Terms for Your Paper*; Generate the Correct Terms for Your Paper; Generate the Correct Terms for Your Paper.

Keywords

similarity measure, incomplete data, web mining

ACM Reference Format:

Yang Cao, Sikun Yang, Kai He, Wenjun Ma, Ming Liu, Yuju Yang, and Jian Weng. 2018. Kernel Representation and Similarity Measure for Incomplete Data. In *Proceedings of Make sure to enter the correct conference title from your rights confirmation email (Conference acronym 'XX)*. ACM, New York, NY, USA, 9 pages. <https://doi.org/XXXXXXX.XXXXXXX>

1 Introduction

The proliferation of web applications has led to an unprecedented growth in data collection from diverse sources, including user interactions, sensor networks, and social media platforms. However, real-world data is inherently incomplete due to various factors such as user privacy preferences, survey non-response and voluntary non-disclosure of information, making the development of robust similarity measures for incomplete data a critical challenge [2].

Measuring similarity between incomplete data samples is a critical problem in web mining and data analysis. Recommendation systems exemplify this challenge: users typically rate only a small fraction of available items, producing highly sparse user-item matrices [9]. The problem intensifies with data heterogeneity, as incompleteness can affect numerical, categorical, or mixed-type features simultaneously. This challenge is critical because similarity measurement serves as the foundation for downstream tasks such as clustering, classification and anomaly detection, where inaccurate similarity estimates can significantly degrade task performance [6].

Traditional approaches to handle missing data in similarity measure fall into several categories. Deletion-based approaches simply ignore missing values or remove incomplete samples entirely. While computationally efficient, these methods suffer from significant information loss and can introduce bias. Imputation-based methods fill missing values using statistical measures (mean, median, mode) or more sophisticated techniques like k-nearest neighbors imputation, matrix factorization, or iterative approaches [11]. However, these approaches often fail to capture the underlying data distribution and may introduce artificial patterns that do not reflect the true similarity structure.

Recent advances have introduced neural network-based approaches for handling missing data, including autoencoders and generative

Permission to make digital or hard copies of all or part of this work for personal or classroom use is granted without fee provided that copies are not made or distributed for profit or commercial advantage and that copies bear this notice and the full citation on the first page. Copyrights for components of this work owned by others than the author(s) must be honored. Abstracting with credit is permitted. To copy otherwise, or republish, to post on servers or to redistribute to lists, requires prior specific permission and/or a fee. Request permissions from permissions@acm.org.

Conference acronym 'XX, Woodstock, NY

© 2018 Copyright held by the owner/author(s). Publication rights licensed to ACM.

ACM ISBN 978-1-4503-XXXX-X/2018/06

<https://doi.org/XXXXXXX.XXXXXXX>

adversarial networks (GANs) that can learn complex data distributions and generate plausible missing values. While promising, these methods typically require large datasets and substantial computational resources, making them less suitable for many web applications where efficiency and interpretability are crucial. Moreover, they often lack theoretical guarantees about the quality of the learned representations and can be sensitive to hyperparameter choices [1].

In this paper, we introduce a novel similarity measure called proximity kernel specifically designed for incomplete data that addresses the limitations of existing approaches. Our method is built on two key innovations: a data dependent binning mechanism combined with proximity assignment, and a cascading fallback strategy that maximizes the utilization of available information for missing value handling.

The binning strategy combined with proximity assignment exhibits data dependent properties: dense regions result in narrower bins with closer quantiles, while sparse regions produce wider bins with more distant quantiles. Through proximity assignment, observed data points are projected into a high-dimensional sparse space via one-hot encoding. This creates an important characteristic where two points in dense regions may have lower similarity than two points in sparse regions, even when their actual distances are comparable, reflecting the local data structure without explicit density estimation.

For missing value handling, we propose a cascading fallback strategy that operates at three levels in the high-dimensional representation space. Rather than imputing values in the original feature space, we estimate the missing encoding as a probability distribution over bins using kernel mean embedding (KME) [15, 16]. First, we seek samples matching across all observed features (intersection-based matching) and use their KME to represent the distribution of missing features. If unsuccessful, we relax to samples matching on any observed feature (union-based matching). Finally, we fall back to global distribution priors. This strategy operates entirely in the representation space, where KME captures the central tendency of distributions without requiring explicit imputation in the original space.

The main contributions of this paper are:

- proposing proximity kernel, a similarity measure that projects data into a high-dimensional sparse representation through equal-frequency binning and Voronoi-based proximity assignment, adapting to local density without explicit density estimation.
- introducing a cascading fallback strategy for missing value handling that progressively relaxes matching constraints from intersection to union to global priors.
- showing that the proposed method achieves linear time complexity, making it scalable to large-scale datasets.
- providing experiments on 12 datasets to demonstrate superior performance over existing methods in clustering tasks.

2 Related Work

Current approaches to similarity measure for incomplete data primarily rely on imputation methods, which can be broadly categorized into traditional statistical techniques and neural network-based approaches.

2.1 Traditional Imputation Methods

Missing data imputation has been extensively studied across various domains. The simplest approach is mean imputation, which replaces missing values with the feature mean for numerical variables or mode for categorical variables [7, 14]. While computationally efficient, this method fails to preserve the natural variability of data and can lead to biased estimates when missing data is not random.

K-nearest neighbors (KNN) [3] imputation estimates missing values based on the average of k most similar complete observations. This approach can capture local patterns but struggles with high-dimensional data and is sensitive to the choice of k and distance metric, often producing poor results when the feature space is sparse.

The Expectation-Maximization (EM) [8] algorithm provides a principled statistical approach to impute missing values based on maximum likelihood density estimation. However, EM requires strong distributional assumptions that may not hold in practice and can converge to local optima.

Multivariate Imputation by Chained Equations (MICE) [19] extends single imputation by creating multiple imputed datasets and combining results to account for imputation uncertainty. MICE can handle mixed-type data and complex missing patterns but requires careful specification of imputation models for each variable and can be computationally expensive.

Tree-based methods like MissForest [17] employ random forests to iteratively impute missing values, leveraging the ensemble nature of random forests to provide robust estimates. MissForest can handle non-linear relationships and mixed-type data but may overfit when the number of variables is large relative to the sample size and lacks theoretical convergence guarantees.

2.2 Deep Learning and Generative Approaches

Recent advances have introduced neural network-based approaches for handling missing data. Generative Adversarial Imputation Networks (GAIN) [20] employs a minimax game between generator and discriminator networks to learn the distribution of missing data. MI-WAE [13] handles missing data by using deep latent variable models and maximises a potentially tight lower bound of the log-likelihood of the observed data. Missing data Imputation Refinement And Causal LEarning (MIRACLE) [12] combines causal inference with deep learning to improve imputation quality by leveraging causal relationships among variables. While deep learning-based methods can produce realistic imputations, they require substantial computational resources and large datasets for stable training.

2.3 Kernel-based Similarity Measure

Traditional similarity measures such as Euclidean distance are not directly applicable to incomplete data. Pairwise deletion simply ignores missing values when computing distances, but this can lead

to biased similarity estimates and significant information loss when missing data is not random.

HI-PMK [21] represents a recent advance in kernel methods for incomplete data. This approach employs a data-dependent kernel that measure the similarity between missing data. While HI-PMK provides a principled way to compute similarities for incomplete observations, it suffers from high computational complexity, requires careful hyperparameter tuning, and may not scale well to large datasets.

3 Preliminary

3.1 Problem Formulation

Let $\mathcal{D} = \{\mathbf{x}_1, \mathbf{x}_2, \dots, \mathbf{x}_n\}$ be a dataset of n samples, where each sample $\mathbf{x}_i \in \mathbb{R}^d$ is a d -dimensional feature vector that may contain missing values. We denote missing values as NaN.

For each sample i , let $O_i \subseteq \{1, 2, \dots, d\}$ be the set of observed feature indices and $M_i = \{1, 2, \dots, d\} \setminus O_i$ be the set of missing feature indices. The observed portion of sample i is $\mathbf{x}_i^{obs} = \{x_{ij} : j \in O_i\}$ and the missing portion is $\mathbf{x}_i^{mis} = \{x_{ij} : j \in M_i\}$.

The goal is to compute a similarity function $s : \mathcal{D} \times \mathcal{D} \rightarrow [0, 1]$ that quantifies the similarity between any two samples \mathbf{x}_i and \mathbf{x}_j , regardless of their missing values. The resulting similarity can be used for downstream tasks such as clustering, where we partition the dataset into K groups based on the computed similarities.

3.2 Kernel Methods

DEFINITION 1 (KERNEL FUNCTION). A kernel function is a symmetric positive definite function $k : \mathcal{X} \times \mathcal{X} \rightarrow \mathbb{R}$ that measures the similarity between two data points in the input space \mathcal{X} .

By Mercer's theorem, any valid kernel function $k(\mathbf{x}, \mathbf{x}')$ can be expressed as an inner product in some reproducing kernel Hilbert space (RKHS) \mathcal{H} :

$$k(\mathbf{x}, \mathbf{x}') = \langle \phi(\mathbf{x}), \phi(\mathbf{x}') \rangle_{\mathcal{H}}, \quad (1)$$

where $\phi : \mathcal{X} \rightarrow \mathcal{H}$ is a feature map that implicitly maps data points from the input space to a potentially infinite-dimensional feature space. This formulation, known as the kernel trick, enables us to compute inner products in \mathcal{H} without explicitly evaluating the feature map ϕ , thereby avoiding the computational burden of working directly in high-dimensional spaces.

3.3 Kernel Mean Embedding

DEFINITION 2 (KERNEL MEAN EMBEDDING). Given a probability distribution P over \mathcal{X} and a kernel function k with associated feature map ϕ , the kernel mean embedding of P is defined as [15, 16]:

$$\mu_P = \mathbb{E}_{\mathbf{x} \sim P}[\phi(\mathbf{x})] \in \mathcal{H}. \quad (2)$$

The kernel mean embedding provides a powerful framework for representing probability distributions as elements in an RKHS. Intuitively, μ_P can be viewed as the "center" of the distribution P when the data points are mapped into the feature space \mathcal{H} via ϕ . This representation maps an entire probability distribution to a single point in the high-dimensional feature space, enabling distribution-level operations through simple vector operations in \mathcal{H} .

For practical applications with finite sample data $\{\mathbf{x}_i\}_{i=1}^n$ drawn i.i.d. from P , the empirical kernel mean embedding is given as:

$$\hat{\mu}_P = \frac{1}{n} \sum_{i=1}^n \phi(\mathbf{x}_i). \quad (3)$$

When the kernel is characteristic (e.g., isolation kernel [18]), the kernel mean embedding is injective, meaning different distributions are mapped to different points in \mathcal{H} , which makes KME a unique and complete representation of distributions.

4 Methodology

Table 1: Key Notations

Notation	Description
X	Data matrix of size $n \times d$
n	Number of samples
d	Number of features
$x_{i,j}$	Value of feature j for sample i
$X_{obs,j}$	Set of observed (non-missing) values for feature j
n_{bins}	Number of bins per feature
$c_{j,k}$	k -th bin center for feature j
k	Bin index, $k \in \{1, 2, \dots, n_{bins}\}$
$b_{i,j}$	Bin assignment for sample i , feature j
$h_{i,j,k}$	k th element of encoding vector $\mathbf{h}_{i,j}$
\mathbf{z}_i	Complete encoding vector for sample i
M_i	Set of missing features for sample i
O_i	Set of observed features for sample i
$C_{i,j}$	Samples matching sample i in feature j
$S_1(i)$	Intersection-based matching samples
$S_2(i)$	Union-based matching samples
$p_{j,k}$	Global prior probability for feature j , bin k
$K(x_i, x_j)$	Proximity kernel between samples x_i and x_j

In this section, we propose proximity kernel that address the challenge of computing meaningful similarities between incomplete data by constructing a data-dependent kernel representation in a high-dimensional space. Given a dataset $X \in \mathbb{R}^{n \times d}$ containing n samples with d features, where missing values are represented as NaN, our goal is to construct a kernel mapping that embeds incomplete data into a reproducing kernel Hilbert space (RKHS) where both imputation and similarity measurement can be performed jointly.

The core insight of our approach is that instead of imputing missing values in the original feature space and then computing similarities, we construct a data-dependent kernel that maps samples to a high-dimensional sparse representation where the geometry naturally reflects the underlying data distribution. This kernel representation exhibits a critical density-adaptive property: *two points in a sparse region are more similar than two points of equal inter-point distance in a dense region*. This property emerges from the combination of equal frequency binning and proximity assignment, making the similarity measure adapt to local density without explicit density estimation.

The proposed proximity kernel consists of four main components: equal-frequency binning that selects density-adaptive bin

centers, proximity assignment that assigns values to nearest bin centers creating Voronoi-like diagram, one-hot encoding that embeds samples into a sparse high-dimensional space, and a cascading fallback strategy that handles missing values through kernel mean embedding principles at progressively relaxed matching levels. The detailed steps are shown as following:

4.1 Data Dependent Binning and Proximity Assignment

4.1.1 Bin Center Selection via Equal-Frequency Binning. For each feature $j \in \{1, 2, \dots, d\}$, we select n_{bins} bin centers using equal-frequency binning. Let $X_{obs,j}$ denote all observed (non-missing) values for feature j . Equal-frequency binning divides the data distribution into n_{bins} intervals, where each interval contains approximately the same number of data points.

The bin centers $c_{j,k}$ are determined by computing evenly-spaced percentiles of the observed distribution:

$$c_{j,k} = \text{percentile} \left(X_{obs,j}, \frac{(k-1) \times 100}{n_{bins}-1} \right), \quad (4)$$

where $k \in \{1, 2, \dots, n_{bins}\}$ is the index of bins.

This yields n_{bins} centers where $c_{j,1}$ and $c_{j,n_{bins}}$ equal the minimum and maximum values of each feature j , and intermediate centers are positioned at equal-frequency intervals.

The equal-frequency approach ensures that bin centers are positioned where data actually exists, adapting automatically to the underlying distribution. *In dense regions where many data points cluster together, consecutive centers are close in value. In sparse regions with few scattered points, consecutive centers are far apart.* This property forms the foundation for density-adaptive behavior without requiring explicit density estimation.

4.1.2 Proximity Assignment Mechanism. Unlike traditional binning methods that assign values to bins based on interval membership, our approach employs proximity assignment. Given the bin centers $\{c_{j,1}, \dots, c_{j,n_{bins}}\}$ for each feature j , we assign each observed value to its nearest center. For sample i and feature j :

$$b_{i,j} = \arg \min_{k \in \{1, \dots, n_{bins}\}} |x_{i,j} - c_{j,k}|, \quad (5)$$

where $b_{i,j} \in \{1, \dots, n_{bins}\}$ denotes the assigned bin index. This proximity assignment creates a Voronoi diagram of the feature space, where each center $c_{j,k}$ defines a Voronoi cell containing all points closer to it than to any other center.

The combination of equal-frequency centers and proximity assignment produces density-adaptive partitioning. Consider two pairs of points with identical Euclidean distance δ : one pair points in a dense region and another in a sparse region. In the dense region, closely-spaced centers create small Voronoi cells, making it more likely that the two points fall into different cells. In the sparse region, widely-spaced centers create large Voronoi cells, making it more likely that the two points fall into the same cell. Figure 1 demonstrates the binning strategy.

4.1.3 One-Hot Encoding Construction. After bin assignment, we encode each feature using one-hot representation. For sample i and each feature j , we construct a binary vector $\mathbf{h}_{i,j} \in \{0, 1\}^{n_{bins}}$:

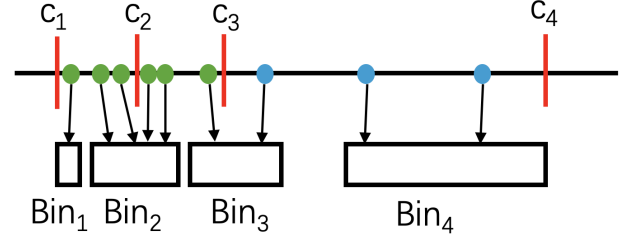


Figure 1: Demonstration of density-adaptive binning. Red lines denote bin centers selected through equal-frequency binning. Green and blue points represent samples in dense and sparse regions, respectively. The sparse region exhibits wider bins compared to the dense region, reflecting the natural adaptation to data distribution without explicit density estimation.

$$h_{i,j,k} = \begin{cases} 1 & \text{if } b_{i,j} = k \\ 0 & \text{otherwise} \end{cases} \quad (6)$$

For example, if a feature is divided into $n_{bins} = 3$ cells. If sample i falls into the first cell for feature j , then $\mathbf{h}_{i,j} = [1, 0, 0]$. The complete encoding for sample i concatenates the one-hot vectors across all features as:

$$\mathbf{z}_i = [\mathbf{h}_{i,1}, \mathbf{h}_{i,2}, \dots, \mathbf{h}_{i,d}]. \quad (7)$$

Continuing the example with $n_{bins} = 3$ and $d = 2$ features, if sample i falls into the first cell for feature 1 and the third cell for feature 2, then $\mathbf{z}_i = [1, 0, 0, 0, 0, 1]$.

For samples without missing values, \mathbf{z}_i is sparse with exactly d ones out of $d \times n_{bins}$ total elements, yielding a sparsity ratio of $\frac{n_{bins}-1}{n_{bins}}$.

4.2 Cascading Fallback Strategy for Missing Value

When sample i contains missing values, we cannot directly apply the proximity assignment and encoding procedures. The core idea is to leverage the observed features to infer which bins the missing features should fall. We identify samples that share similar patterns in their observed features, and use kernel mean embedding over these similar samples to estimate the missing feature distributions.

Let $M_i = \{j : x_{i,j} = \text{NaN}\}$ denote the set of missing features for sample i , and $O_i = \{1, \dots, d\} \setminus M_i$ denote the observed features. We employ a three-level cascading strategy that progressively relaxes the matching criteria when stricter criteria fail to find similar samples.

4.2.1 Level 1: Intersection-Based Exact Matching. The first level seeks samples that match sample i on all observed features. For each observed feature $j \in O_i$, we identify the set $C_{i,j}$ of all other samples (indexed by m) that fall into the same bin as sample i :

$$C_{i,j} = \{m : m \neq i, b_{m,j} = b_{i,j}\}, \quad (8)$$

The intersection-based matching set $S_i(i)$ is the intersection across all observed features:

$$S_i(i) = \bigcap_{j \in O_i} C_{i,j}. \quad (9)$$

This set contains all samples (excluding sample i itself) that have been assigned to the same bins as sample i for each observed feature. If $S_1(i) \neq \emptyset$, we estimate missing encoding through kernel mean embedding:

$$h_{i,j,k} = \frac{1}{|S_1(i)|} \sum_{m \in S_1(i)} h_{m,j,k}, \quad \forall j \in M_i, k = 1, \dots, n_{bins}. \quad (10)$$

This averaging process is essentially a kernel mean embedding operation that produces values between 0 and 1, representing the empirical probability distribution over bins for each missing feature based on the patterns observed in similar samples.

4.2.2 Level 2: Union-Based Partial Matching. In practice, the intersection $S_1(i)$ may be empty, particularly when the sample exhibits a rare combination of feature values. When no samples match across all observed features simultaneously, we cannot apply the intersection-based estimation. To provide a robust fallback mechanism, we relax the constraint to consider samples that match on any observed feature.

We define the union-based matching set as:

$$S_2(i) = \bigcup_{j \in O_i} C_{i,j}. \quad (11)$$

This set contains all samples that share at least one Voronoi cell with sample i in any observed feature. The union operation aggregates samples with partial similarity rather than requiring complete agreement. If $S_2(i) \neq \emptyset$, we apply kernel mean embedding over this broader set:

$$h_{i,j,k} = \frac{1}{|S_2(i)|} \sum_{m \in S_2(i)} h_{m,j,k}, \quad \forall j \in M_i, k = 1, \dots, n_{bins}. \quad (12)$$

The key distinction from Level 1 is the relaxation of matching criteria. Level 1 seeks samples with identical patterns across all observed features, providing high-confidence estimates but potentially finding no matches. Level 2 trades specificity for coverage, utilizing information from any partially similar samples.

4.2.3 Level 3: Global Prior Distribution. Even the union-based matching may fail to find any similar samples. This occurs when sample i occupies Voronoi cells that no other samples occupy in any of its observed features, which can happen with outliers, samples in sparse regions, or datasets with high-dimensional sparse patterns. When $S_2(i) = \emptyset$, we cannot leverage local similarity and must use the global distribution of each missing feature.

For each missing feature $j \in M_i$ and each bin k , we compute the probability:

$$p_{j,k} = \frac{\text{count of samples in bin } k \text{ for feature } j}{\text{count of samples with observed feature } j}. \quad (13)$$

The missing encoding is set to this probability distribution:

$$\mathbf{h}_{i,j} = [p_{j,1}, p_{j,2}, \dots, p_{j,n_{bins}}], \quad (14)$$

where $\sum_{k=1}^{n_{bins}} p_{j,k} = 1$. For example, if 50% of samples fall in bin 1, 30% in bin 2, and 20% in bin 3 for feature j , then $\mathbf{h}_{i,j} = [0.5, 0.3, 0.2]$, representing the probability distribution over bins.

This strategy simply treats each feature as if it were unrelated to the observed features. The global prior acts as the final safety mechanism, guaranteeing that every sample receives a valid encoding even when no similar samples exist.

4.3 Kernel Representation and Similarity Measure

The encoding vectors $\mathbf{z}_i \in [0, 1]^{d \times n_{bins}}$ form a sparse kernel representation. For complete data, these are binary; for incomplete data with estimated features, they contain fractional values from the cascading fallback strategy.

We define the proximity kernel between samples m and n as:

$$K(x_m, x_n) = \frac{1}{d} \mathbf{z}_m^T \mathbf{z}_n = \langle \mathbf{z}_m, \mathbf{z}_n \rangle. \quad (15)$$

This similarity measure has a probabilistic interpretation: it computes the expected probability that two samples fall into the same bin, averaged across all features. For each feature, if both samples occupy the same Voronoi cell (same bin), they contribute 1 to the inner product; otherwise they contribute 0. The normalization by d yields the average co-occurrence rate across all features.

The proximity kernel satisfies $K(x_m, x_n) \in [0, 1]$:

- $K(x_m, x_n) = 1$ indicates perfect similarity (co-occurrence in all features).
- $K(x_m, x_n) = 0$ indicates complete dissimilarity (no co-occurrence).
- Intermediate values represent the fraction of features where samples co-occur.

For samples with missing values, the fractional encodings naturally integrate into this framework. The inner product $\mathbf{z}_i^T \mathbf{z}_j$ computes the sum of element-wise products, where fractional values from kernel mean embedding represent probability distributions over bins.

The sparse kernel representation \mathbf{z}_i serves dual purposes: it enables similarity computation through the proximity kernel, and it can be used directly as input features for downstream machine learning tasks such as clustering, classification, or dimensionality reduction on incomplete data.

4.4 Kernel Validity Proof

The proximity kernel $K(x_i, x_j)$ is constructed as an inner product in the representation space. We verify that this construction yields a valid kernel by demonstrating it satisfies Mercer's conditions: symmetry and positive semi-definiteness [4].

Proof of Positive Semi-Definiteness: Consider the gram matrix $\mathbf{K} \in \mathbb{R}^{n \times n}$ with entries $K_{ij} = K(x_i, x_j)$ for samples x_1, \dots, x_n . Let $\mathbf{Z} \in \mathbb{R}^{n \times (d \times n_{bins})}$ be the matrix where each row is a sample representation \mathbf{z}_i . The gram matrix can be expressed as:

$$\mathbf{K} = \frac{1}{d} \mathbf{Z} \mathbf{Z}^T. \quad (16)$$

The matrix $\mathbf{Z} \mathbf{Z}^T$ is a Gram matrix whose (i, j) -th entry equals $\mathbf{z}_i^T \mathbf{z}_j$. Gram matrices are positive semi-definite, and scaling by the positive constant $\frac{1}{d}$ preserves this property.

To verify, for any coefficient vector $\boldsymbol{\alpha} = [\alpha_1, \dots, \alpha_n]^T$:

$$\boldsymbol{\alpha}^T \mathbf{K} \boldsymbol{\alpha} = \frac{1}{d} \boldsymbol{\alpha}^T \mathbf{Z} \mathbf{Z}^T \boldsymbol{\alpha} = \frac{1}{d} \|\mathbf{Z}^T \boldsymbol{\alpha}\|^2 \geq 0. \quad (17)$$

Proof of Symmetry: The inner product operation is commutative:

$$\begin{aligned} K(x_i, x_j) &= \langle \mathbf{z}_i, \mathbf{z}_j \rangle \\ &= \langle \mathbf{z}_j, \mathbf{z}_i \rangle \\ &= K(x_j, x_i). \end{aligned} \quad (18)$$

Having established both properties, the proximity kernel satisfies Mercer’s conditions and defines a valid reproducing kernel Hilbert space.

Implications for Kernel Methods: The validity of the proximity kernel enables its use in kernel-based algorithms. When representations \mathbf{z}_i serve as features in k-means clustering, the algorithm minimizes:

$$\arg \min_{\text{clusters}} \sum_i \|\mathbf{z}_i - \boldsymbol{\mu}_c\|^2, \quad (19)$$

where $\boldsymbol{\mu}_c$ is the cluster centroid. Expanding the squared distance shows that this objective depends on kernel values $K(x_i, x_j)$, making k-means in representation space equivalent to a kernel-based clustering approach.

4.5 Summary

The proposed proximity kernel can be summarized as follows:

- (1) Bin Center Selection: For each feature j , compute equal-frequency-based bin centers using observed values only.
- (2) Proximity Assignment: Assign each observed value to its nearest bin center.
- (3) One-Hot Encoding: Create binary encodings for observed features.
- (4) Missing Value Handling: Apply the cascading fallback strategy using KME at each level.

5 Experiments

5.1 Experimental Settings

Datasets: We evaluate the proximity kernel on 12 real-world datasets with varying characteristics. The datasets span multiple domains including medical diagnosis (Kidney, Hepatitis, Heart, Tumor, Cancer), biological classification (Soybean, Mushroom), financial analysis (Credit), demographic prediction (Adult), political analysis (Voting), and others (Mammography, Horse). These datasets exhibit diverse properties in terms of sample size and feature dimensionality, providing a comprehensive testbed for evaluating incomplete data methods. Table 2 shows the statistical information of datasets. All of these datasets are from UCI datasets ¹.

Baselines: We compare 9 representative methods: (1) Simple imputation: Mean imputation; (2) Statistical methods: MissForest, MICE, KNN, EM; (3) Deep learning approaches: GAIN, MIRACLE, MIWAE; (4) Kernel-based method: HI-PMK. These baselines cover the spectrum from classical to state-of-the-art techniques for handling incomplete data. The code of them are from python library scikit-learn ² and hyperimpute ³ [10].

Evaluation Protocol: Following standard practice, we evaluate all methods on clustering quality using Normalized Mutual Information (NMI) as the metric. For fair comparison, we applied K-means with the number of clusters to the ground-truth number of classes.

¹<https://archive.ics.uci.edu/datasets>

²<https://scikit-learn.org/stable/modules/impute.html>

³<https://hyperimpute.readthedocs.io/en/latest/>

Table 2: Statistical information of datasets

Dataset	# Samples	# Dim.	# Cat.	# Num.	# Missing	Class
Kidney	400	25	3	22	10.54	2
Mammo	961	5	0	4	3.37	2
Heart	303	13	7	6	0.15	5
Hepatitis	155	19	13	6	5.67	2
Horse	368	27	0	27	19.39	2
Cancer	699	9	1	8	0.25	2
Credit	690	15	9	6	0.64	2
Adult	48842	14	7	7	0.32	4
Voting	435	16	16	0	5.63	2
Mushroom	8124	22	21	1	1.39	2
Tumor	339	17	0	17	3.90	21
Soybean	307	35	35	0	6.63	19

Each experiment was conducted 10 times and report average results for stability.

Hyperparameter Settings: To ensure fair comparison, we perform hyperparameter tuning for all baseline methods. MissForest is configured with mean as initial guess and maximum iterations searched over $\{5, 10, 15\}$. MICE explores maximum iterations in $\{10, 100, 200, 500\}$. KNN imputation searches the number of neighbors in $\{5, 10, 20\}$. The EM algorithm tunes maximum iterations over $\{10, 100, 200, 500\}$. For deep learning methods, GAIN searches training epochs in $\{100, 200, 500\}$, MIRACLE tunes learning rate over $\{0.001, 0.0001, 0.00001\}$, MIWAE explores epochs in $\{100, 200, 500\}$, and they use the same batch size in $\{32, 64, 128, 256\}$. For the proximity kernel, we search the number of bins per dimension in $\{2, 3, 4, 6, 8\}$.

5.2 Empirical Evaluation

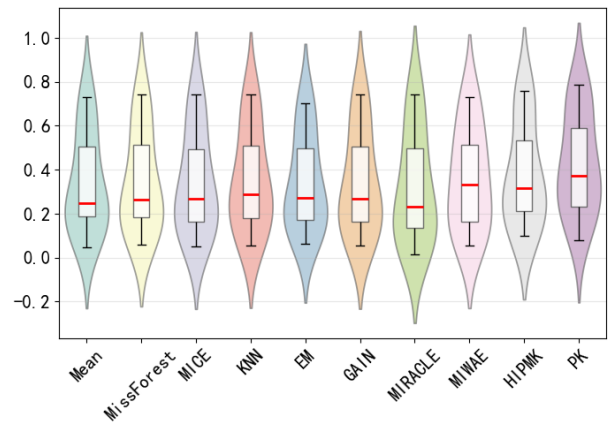


Figure 2: Comparison of all methods performance in terms of NMI.

Figure 2 presents the performance comparison using box and violin plots. The boxplots highlight a clear performance hierarchy, with the proposed method achieving the highest median. The violin plots reveal the shape of the performance distributions: PK is concentrated in the high-performance region, whereas several baseline methods display broader distributions, with significant

Table 3: Results between baselines and proposed methods in terms of NMI. The best performance are in bold.

Data	Kidney	Mammo	Heart	Hepatitis	Horse	Wiscom	Credit	Adult	Voting	M.room	Tumor	Soybean	AVG.
Mean	0.5457	0.2584	0.1660	0.1932	<u>0.2350</u>	0.7315	0.2101	0.0477	0.4935	0.1114	0.3679	0.7008	0.3384
MissForest	0.5597	0.264	0.1699	0.1978	0.1900	0.7427	0.2612	0.0605	<u>0.4958</u>	0.0905	0.3728	0.7040	0.3424
MICE	0.5473	0.2624	0.1724	0.2082	0.1358	0.7427	0.2756	0.0506	0.4773	0.0957	0.3700	0.7061	0.3370
KNN	<u>0.5696</u>	0.2636	0.1651	0.1861	0.2586	0.7427	0.3095	0.0542	0.4903	0.0799	0.3726	0.7145	0.3506
EM	0.5405	0.2693	0.1652	0.1739	0.1860	0.7039	0.2717	0.0638	0.4852	0.1213	0.3687	0.6954	0.3371
GAIN	0.5593	0.2723	0.1651	0.1989	0.1600	0.7427	0.2668	0.0729	0.4895	0.0556	0.3678	0.7134	0.3387
MIRACLE	0.5385	0.2633	0.1985	0.1590	0.0147	0.7427	0.1582	0.0728	0.4840	0.0556	0.3653	0.7370	0.3158
MIWAE	0.5522	0.2897	0.1638	0.1590	0.2130	0.7295	0.4279	0.0680	0.5012	0.0559	0.3737	0.7137	0.3540
HI-PMK	0.6663	<u>0.3271</u>	<u>0.2142</u>	0.2001	0.1006	<u>0.7585</u>	0.2316	0.0987	0.4892	<u>0.3061</u>	0.3872	<u>0.7478</u>	0.3773
Ours	0.6964	0.3315	0.2323	0.2289	0.1911	0.785	<u>0.3698</u>	<u>0.0791</u>	0.4947	0.554	<u>0.3774</u>	0.7514	0.4245

mass extending into lower-performance ranges. This indicates that our method not only attains superior average performance but also maintains greater consistency across datasets with varying characteristics.

Table 3 presents the full results across 12 datasets. The proposed method achieves the best or second-best performance on 10 out of 12 datasets, and obtains the highest average NMI across all datasets. The superior and stable performance of the proximity kernel highlights the effectiveness of computing similarity directly in the kernel representation space through the cascading fallback strategy, rather than relying on explicit imputation in the original feature space followed by separate similarity computation.

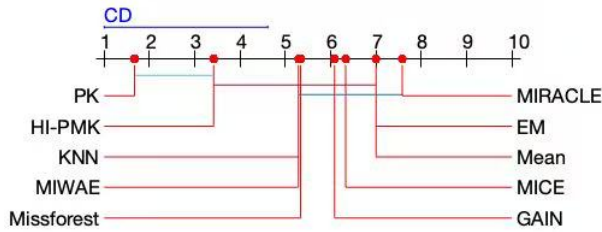


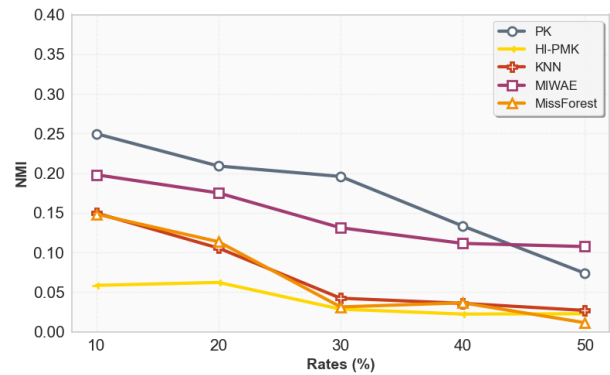
Figure 3: Friedman-Nemenyi test at significance level 0.1. If two algorithms are connected by a CD (critical difference) line, there is no significant difference between them.

The critical difference diagrams in Figure 3 provide Friedman-Nemenyi test [5] at significance level 0.1. PK is the only method that shows significant better performance than all methods except HI-PMK. This establishes the statistical superiority and robustness of the proposed approach across different datasets.

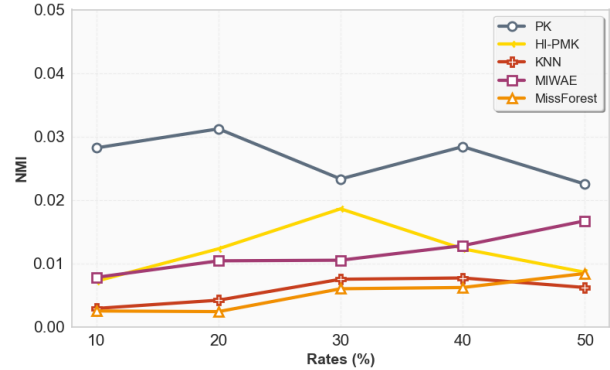
5.3 Missing Rate Handling

To evaluate the robustness of PK under varying degrees of data incompleteness, we conduct experiments on two non-missing datasets (3L and Messidor). We systematically generate missing data at different rates ranging from 10% to 50% using the Missing Completely At Random (MCAR) mechanism, where each value has an equal probability of being missing independent of both observed and unobserved data. This controlled experimental setup allows us to isolate the impact of missing rate on algorithm performance.

Figure 4 presents the clustering performance measured by NMI across different missing rates for both datasets. On the 3L dataset



(a) 3L



(b) Messidor

Figure 4: Clustering performance of top 5 methods under different missing rates on 3L and Messidor datasets.

(Figure 4a), the proposed PK method maintains superior and relatively stable performance across low to moderate missing rates (10%-40%). Baseline methods such as KNN and MissForest exhibit steeper performance degradation, with their NMI scores dropping to near-zero by 30% missing rate, indicating a complete loss of clustering quality. While most baseline methods struggle significantly as the missing rate increases, MIWAE shows competitive performance and slightly outperforms PK at the 50% missing rate. The proposed method demonstrates greater resilience, sustaining

reasonable performance even at higher missing rates. However, this marginal advantage comes at a significantly higher computational cost, MIWAE requires iterative neural network training with multiple epochs, while PK operates with linear time complexity through a single-pass algorithm.

On the Messidor dataset (Figure 4b), the proposed method gets best performance on all rates. At the extreme 50% missing rate, all methods face substantial challenges due to severe information loss, with performance metrics declining across the board. Nevertheless, PK maintains a favorable efficiency-performance trade-off compared to computationally expensive deep learning approaches. The cascading fallback strategy proves effective in leveraging available information even when half of the data is missing, gradually relaxing from intersection-based matching to union-based matching and finally to global priors as the missing rate increases.

5.4 Scalability Analysis

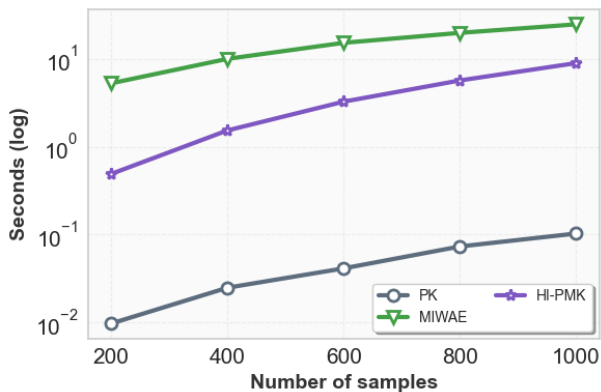


Figure 5: Runtime comparison between PK, MIWAE and HI-PMK.

We analyze the computational complexity of the proximity kernel in terms of both time and space requirements.

Time Complexity: PK consists of three main phases. The bin center selection phase computes percentiles for each feature, requiring $O(n \log n)$ time for sorting observed values per feature, yielding $O(d \cdot n \log n)$ overall. The encoding phase assigns each observed value to its nearest bin center in $O(n_{bins})$ time per value, resulting in $O(n \cdot d \cdot n_{bins})$ complexity. Since n_{bins} is a small constant (typically 3-10), this is effectively $O(nd)$. The missing value handling phase has worst-case complexity $O(n^2 d)$ when union-based matching is frequently required. However, in practice, intersection-based matching succeeds for most samples, reducing the average complexity significantly. Overall, the time complexity is $O(nd + d \cdot n \log n)$, which is linear in the number of samples for fixed dimensionality.

Figure 5 presents a comparison of the running time for PK, HI-PMK, and MIWAE, where HI-PMK and MIWAE represent the best-performing traditional and deep learning methods, respectively. The results demonstrate that PK is significantly faster than both competing methods.

Space Complexity: The method requires $O(d \cdot n_{bins})$ space to store bin centers, $O(n \cdot d \cdot n_{bins})$ space for the encoded representations, and $O(n_{bins} \cdot d)$ space for global priors. Since n_{bins} is a small constant, the space complexity is effectively $O(nd)$, linear in both the number of samples and features. The sparse nature of the representation (sparsity ratio $\frac{n_{bins}-1}{n_{bins}}$) enables efficient storage and computation.

Practical Scalability: The linear scaling in sample size makes the proximity kernel suitable for large-scale applications. Unlike methods requiring iterative optimization (EM, MICE) or expensive neural network training (GAIN, MIWAE), the proximity kernel computes representations in a single pass after the initial bin center selection. The representation construction is parallel across samples, allowing for straightforward distributed implementation for web-scale datasets.

5.5 Sensitivity Analysis

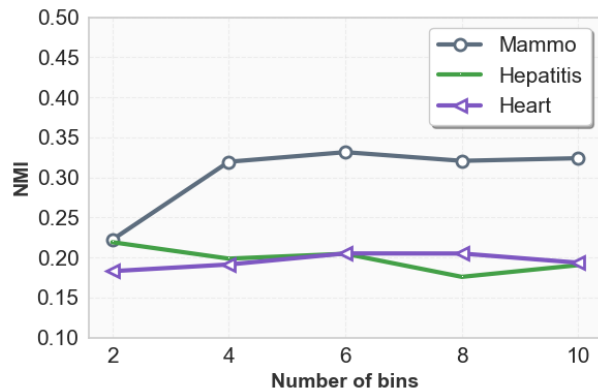


Figure 6: Performance under different number of bins.

The proximity kernel method has a single hyperparameter: the number of bins per feature (n_{bins}). Figure 6 presents the clustering performance (NMI) across three datasets (Mammo, Hepatitis, and Heart) as the number of bins varies from 2 to 10.

The results demonstrate that the proximity kernel exhibits stable performance across different bin configurations. For the Mammo dataset, NMI scores fluctuate only slightly between 0.30 and 0.33 across all tested bin numbers. Similarly, the Heart and Hepatitis datasets maintain consistent performance around 0.18-0.2 and 0.17-0.21, respectively. This stability indicates that the proposed method is robust to hyperparameter choices and does not require extensive tuning to achieve good performance.

In practice, we found that n_{bins} values between 3 and 6 provide a good balance between representation granularity and computational efficiency. Too few bins ($n_{bins} = 2$) may result in overly coarse discretization, while too many bins may lead to sparse representations without meaningful performance gains.

This robustness contrasts with many baseline methods that require careful tuning of multiple hyperparameters, such as the number of neighbors in KNN, learning rates and epochs in deep learning approaches, or iterations in EM and MICE. The minimal parameterization makes the proximity kernel particularly suitable for

large-scale applications where extensive hyperparameter search may be impractical.

6 Discussion and Conclusion

This paper presents proximity kernel, a novel similarity measure for incomplete data that integrates data dependent binning with a cascading fallback strategy. Unlike existing two-stage approaches that separate imputation from similarity computation, our method jointly handles missing values through kernel mean embedding over progressively relaxed matching criteria, from intersection-based to union-based to global priors. The equal-frequency binning combined with proximity assignment creates partitions that adapt to data density, while the resulting kernel representation is proven to be positive semi-definite and valid for kernel-based algorithms. Experimental results on 12 datasets demonstrate that the proximity kernel achieves superior performance with linear time complexity, making it suitable for large-scale web applications.

It is worth noting that the current evaluation focuses on the Missing Completely At Random (MCAR) mechanism, where missingness is independent of both observed and unobserved values. Real-world data often exhibits more complex missing patterns, such as Missing At Random (MAR) and Missing Not At Random (MNAR). Investigating the proximity kernel's behavior under these more challenging scenarios represents an important direction for future work, along with exploring adaptive bin selection strategies and establishing theoretical convergence guarantees for the cascading fallback mechanism.

References

- [1] Deepak Adhikari, Wei Jiang, Jinyu Zhan, Zhiyuan He, Danda B Rawat, Uwe Aickelin, and Hadi A Khorshidi. 2022. A comprehensive survey on imputation of missing data in internet of things. *Comput. Surveys* 55, 7 (2022), 1–38.
- [2] Douglas G Altman and J Martin Bland. 2007. Missing data. *Bmj* 334, 7590 (2007), 424–424.
- [3] Naomi S Altman. 1992. An introduction to kernel and nearest-neighbor nonparametric regression. *The American Statistician* 46, 3 (1992), 175–185.
- [4] Andreas Christmann and Ingo Steinwart. 2008. Support vector machines. (2008).
- [5] Janez Demšar. 2006. Statistical comparisons of classifiers over multiple data sets. *Journal of Machine learning research* 7, Jan (2006), 1–30.
- [6] Tlameo Emmanuel, Thabiso Maupong, Dimane Mpoeleng, Thabo Semong, Banyatsang Mphago, and Oteng Tabona. 2021. A survey on missing data in machine learning. *Journal of Big data* 8, 1 (2021), 140.
- [7] Alireza Farhangfar, Lukasz A Kurgan, and Witold Pedrycz. 2007. A novel framework for imputation of missing values in databases. *IEEE Transactions on Systems, Man, and Cybernetics-Part A: Systems and Humans* 37, 5 (2007), 692–709.
- [8] Zoubin Ghahramani and Michael Jordan. 1993. Supervised learning from incomplete data via an EM approach. *Advances in neural information processing systems* 6 (1993).
- [9] Gökhan Göksel, Ahmet Aydın, Zeynep Batmaz, and Cihan Kaleli. 2025. A novel missing value imputation for multi-criteria recommender systems. *Information Sciences* 712 (2025), 122139.
- [10] Daniel Jarrett, Bogdan Cebere, Tennison Liu, Alicia Curth, and Mihaela van der Schaar. 2022. HyperImpute: Generalized Iterative Imputation with Automatic Model Selection. (2022). doi:10.48550/ARXIV.2206.07769
- [11] Jae Kwang Kim and Jun Shao. 2021. *Statistical methods for handling incomplete data*. Chapman and Hall/CRC.
- [12] Trent Kyono, Yao Zhang, Alexis Bellot, and Mihaela van der Schaar. 2021. Miracle: Causally-aware imputation via learning missing data mechanisms. *Advances in Neural Information Processing Systems* 34 (2021), 23806–23817.
- [13] Pierre-Alexandre Mattei and Jes Frellesen. 2019. MIWAE: Deep generative modelling and imputation of incomplete data sets. In *International conference on machine learning*. PMLR, 4413–4423.
- [14] Xiaoye Miao, Yangyang Wu, Lu Chen, Yunjun Gao, and Jianwei Yin. 2022. An experimental survey of missing data imputation algorithms. *IEEE Transactions on Knowledge and Data Engineering* 35, 7 (2022), 6630–6650.
- [15] Krikamol Muandet, Kenji Fukumizu, Bharath Sriperumbudur, Bernhard Schölkopf, et al. 2017. Kernel mean embedding of distributions: A review and beyond. *Foundations and Trends® in Machine Learning* 10, 1-2 (2017), 1–141.
- [16] Alex Smola, Arthur Gretton, Le Song, and Bernhard Schölkopf. 2007. A Hilbert space embedding for distributions. In *International conference on algorithmic learning theory*. Springer, 13–31.
- [17] Daniel J Stekhoven and Peter Bühlmann. 2012. MissForest—non-parametric missing value imputation for mixed-type data. *Bioinformatics* 28, 1 (2012), 112–118.
- [18] Kai Ming Ting, Yue Zhu, and Zhi-Hua Zhou. 2018. Isolation kernel and its effect on SVM. In *Proceedings of the 24th ACM SIGKDD international conference on knowledge discovery & data mining*. 2329–2337.
- [19] Stef Van Buuren and Karin Groothuis-Oudshoorn. 2011. mice: Multivariate imputation by chained equations in R. *Journal of statistical software* 45 (2011), 1–67.
- [20] Jinsung Yoon, James Jordon, and Mihaela Schaar. 2018. Gain: Missing data imputation using generative adversarial nets. In *International conference on machine learning*. PMLR, 5689–5698.
- [21] Youran Zhou, Mohamed Reda Bouadjene, Jonathan Wells, and Sunil Arya. 2025. Handling Incomplete Heterogeneous Data using a Data-Dependent Kernel. *arXiv preprint arXiv:2501.04300* (2025).